

Search for New Particles Decaying to Dijets in $p\bar{p}$ Collisions at $\sqrt{s} = 1.8$ TeV

F. Abe,¹³ M. G. Albrow,⁷ S. R. Amendolia,²³ D. Amidei,¹⁶ J. Antos,²⁸ C. Anway-Wiese,⁴ G. Apollinari,²⁶ H. Areti,⁷ M. Atac,⁷ P. Auchincloss,²⁵ F. Azfar,²¹ P. Azzi,²⁰ N. Bacchetta,¹⁸ W. Badgett,¹⁶ M. W. Bailey,¹⁸ J. Bao,³⁵ P. de Barbaro,²⁵ A. Barbaro-Galtieri,¹⁴ V. E. Barnes,²⁴ B. A. Barnett,¹² P. Bartalini,²³ G. Bauer,¹⁵ T. Baumann,⁹ F. Bedeschi,²³ S. Behrends,³ S. Belforte,²³ G. Bellettini,²³ J. Bellinger,³⁴ D. Benjamin,³¹ J. Benlloch,¹⁵ J. Bensinger,³ D. Benton,²¹ A. Beretvas,⁷ J. P. Berge,⁷ S. Bertolucci,⁸ A. Bhatti,²⁶ K. Biery,¹¹ M. Binkley,⁷ F. Bird,²⁹ D. Bisello,²⁰ R. E. Blair,¹ C. Blocker,³ A. Bodek,²⁵ W. Bokhari,¹⁵ V. Bolognesi,²³ D. Bortoletto,²⁴ C. Boswell,¹² T. Boulos,¹⁴ G. Brandenburg,⁹ C. Bromberg,¹⁷ E. Buckley-Geer,⁷ H. S. Budd,²⁵ K. Burkett,¹⁶ G. Busetto,²⁰ A. Byon-Wagner,⁷ K. L. Byrum,¹ J. Cammerata,¹² C. Campagnari,⁷ M. Campbell,¹⁶ A. Caner,⁷ W. Carithers,¹⁴ D. Carlsmith,³⁴ A. Castro,²⁰ Y. Cen,²¹ F. Cervelli,²³ H. Y. Chao,²⁸ J. Chapman,¹⁶ M.-T. Cheng,²⁸ G. Chiarelli,⁸ T. Chikamatsu,³² C. N. Chiou,²⁸ S. Cihangir,⁷ A. G. Clark,²³ M. Cobal,²³ M. Contreras,⁵ J. Conway,²⁷ J. Cooper,⁷ M. Cordelli,⁸ C. Couyoumtzelis,²³ D. Crane,¹ J. D. Cunningham,³ T. Daniels,¹⁵ F. DeJongh,⁷ S. Delchamps,⁷ S. Dell'Agnello,²³ M. Dell'Orso,²³ L. Demortier,²⁶ B. Denby,²³ M. Deninno,² P. F. Derwent,¹⁶ T. Devlin,²⁷ M. Dickson,²⁵ J. R. Dittmann,⁶ S. Donati,²³ R. B. Drucker,¹⁴ A. Dunn,¹⁶ K. Einsweiler,¹⁴ J. E. Elias,⁷ R. Ely,¹⁴ E. Engels, Jr.,²² S. Eno,⁵ D. Errede,¹⁰ S. Errede,¹⁰ Q. Fan,²⁵ B. Farhat,¹⁵ I. Fiori,² B. Flaughner,⁷ G. W. Foster,⁷ M. Franklin,⁹ M. Frautschi,¹⁸ J. Freeman,⁷ J. Friedman,¹⁵ H. Frisch,⁵ A. Fry,²⁹ T. A. Fuess,¹ Y. Fukui,¹³ S. Funaki,³² G. Gagliardi,²³ S. Galeotti,²³ M. Gallinaro,²⁰ A. F. Garfinkel,²⁴ S. Geer,⁷ D. W. Gerdes,¹⁶ P. Giannetti,²³ N. Giokaris,²⁶ P. Giromini,⁸ L. Gladney,²¹ D. Glenzinski,¹² M. Gold,¹⁸ J. Gonzalez,²¹ A. Gordon,⁹ A. T. Goshaw,⁶ K. Goulianos,²⁶ H. Grassmann,⁶ A. Grewal,²¹ G. Grieco,²³ L. Groer,²⁷ C. Grosso-Pilcher,⁵ C. Haber,¹⁴ S. R. Hahn,⁷ R. Hamilton,⁹ R. Handler,³⁴ R. M. Hans,³⁵ K. Hara,³² B. Harral,²¹ R. M. Harris,⁷ S. A. Hauger,⁶ J. Hauser,⁴ C. Hawk,²⁷ J. Heinrich,²¹ D. Cronin-Hennessy,⁶ R. Hollebeek,²¹ L. Holloway,¹⁰ A. Hölscher,¹¹ S. Hong,¹⁶ G. Houk,²¹ P. Hu,²² B. T. Huffman,²² R. Hughes,²⁵ P. Hurst,⁹ J. Huston,¹⁷ J. Huth,⁹ J. Hylen,⁷ M. Incagli,²³ J. Incandela,⁷ H. Iso,³² H. Jensen,⁷ C. P. Jessop,⁹ U. Joshi,⁷ R. W. Kadel,¹⁴ E. Kajfasz,^{7a} T. Kamon,³⁰ T. Kaneko,³² D. A. Kardelis,¹⁰ H. Kasha,³⁵ Y. Kato,¹⁹ L. Keeble,⁸ R. D. Kennedy,²⁷ R. Kephart,⁷ P. Kesten,¹⁴ D. Kestenbaum,⁹ R. M. Keup,¹⁰ H. Keutelian,⁷ F. Keyvan,⁴ D. H. Kim,⁷ H. S. Kim,¹¹ S. B. Kim,¹⁶ S. H. Kim,³² Y. K. Kim,¹⁴ L. Kirsch,³ P. Koehn,²⁵ K. Kondo,³² J. Konigsberg,⁹ S. Kopp,⁵ K. Kordas,¹¹ W. Koska,⁷ E. Kovacs,^{7a} W. Kowald,⁶ M. Krasberg,¹⁶ J. Kroll,⁷ M. Kruse,²⁴ S. E. Kuhlmann,¹ E. Kuns,²⁷ A. T. Laasanen,²⁴ N. Labanca,²³ S. Lammel,⁴ J. I. Lamoureux,³ T. LeCompte,¹⁰ S. Leone,²³ J. D. Lewis,⁷ P. Limon,⁷ M. Lindgren,⁴ T. M. Liss,¹⁰ N. Lockyer,²¹ C. Loomis,²⁷ O. Long,²¹ M. Loretì,²⁰ E. H. Low,²¹ J. Lu,³⁰

D. Lucchesi,²³ C. B. Luchini,¹⁰ P. Lukens,⁷ P. Maas,³⁴ K. Maeshima,⁷ A. Maghakian,²⁶ P. Maksimovic,¹⁵ M. Mangano,²³ J. Mansour,¹⁷ M. Mariotti,²³ J. P. Marriner,⁷ A. Martin,¹⁰ J. A. J. Matthews,¹⁸ R. Mattingly,¹⁵ P. McIntyre,³⁰ P. Melese,²⁶ A. Menzione,²³ E. Meschi,²³ G. Michail,⁹ S. Mikamo,¹³ M. Miller,⁵ R. Miller,¹⁷ T. Mimashi,³² S. Miscetti,⁸ M. Mishina,¹³ H. Mitsushio,³² S. Miyashita,³² Y. Morita,¹³ S. Moulding,²⁶ J. Mueller,²⁷ A. Mukherjee,⁷ T. Muller,⁴ P. Musgrave,¹¹ L. F. Nakaie,²⁹ I. Nakano,³² C. Nelson,⁷ D. Neuberger,⁴ C. Newman-Holmes,⁷ L. Nodulman,¹ S. Ogawa,³² S. H. Oh,⁶ K. E. Ohl,³⁵ R. Oishi,³² T. Okusawa,¹⁹ C. Pagliarone,²³ R. Paoletti,²³ V. Papadimitriou,³¹ S. Park,⁷ J. Patrick,⁷ G. Pauletta,²³ M. Paulini,¹⁴ L. Pescara,²⁰ M. D. Peters,¹⁴ T. J. Phillips,⁶ G. Piacentino,² M. Pillai,²⁵ R. Plunkett,⁷ L. Pondrom,³⁴ N. Produit,¹⁴ J. Proudfoot,¹ F. Ptohos,⁹ G. Punzi,²³ K. Ragan,¹¹ F. Rimondi,² L. Ristori,²³ M. Roach-Bellino,³³ W. J. Robertson,⁶ T. Rodrigo,⁷ J. Romano,⁵ L. Rosenson,¹⁵ W. K. Sakumoto,²⁵ D. Saltzberg,⁵ A. Sansoni,⁸ V. Scarpine,³⁰ A. Schindler,¹⁴ P. Schlabach,⁹ E. E. Schmidt,⁷ M. P. Schmidt,³⁵ O. Schneider,¹⁴ G. F. Sciacca,²³ A. Scribano,²³ S. Segler,⁷ S. Seidel,¹⁸ Y. Seiya,³² G. Sganos,¹¹ A. Sgolacchia,² M. Shapiro,¹⁴ N. M. Shaw,²⁴ Q. Shen,²⁴ P. F. Shepard,²² M. Shimojima,³² M. Shochet,⁵ J. Siegrist,²⁹ A. Sill,³¹ P. Sinervo,¹¹ P. Singh,²² J. Skarha,¹² K. Sliwa,³³ D. A. Smith,²³ F. D. Snider,¹² L. Song,⁷ T. Song,¹⁶ J. Spalding,⁷ L. Spiegel,⁷ P. Sphicas,¹⁵ A. Spies,¹² L. Stanco,²⁰ J. Steele,³⁴ A. Stefanini,²³ K. Strahl,¹¹ J. Strait,⁷ D. Stuart,⁷ G. Sullivan,⁵ K. Sumorok,¹⁵ R. L. Swartz, Jr.,¹⁰ T. Takahashi,¹⁹ K. Takikawa,³² F. Tartarelli,²³ W. Taylor,¹¹ P. K. Teng,²⁸ Y. Teramoto,¹⁹ S. Tether,¹⁵ D. Theriot,⁷ J. Thomas,²⁹ T. L. Thomas,¹⁸ R. Thun,¹⁶ M. Timko,³³ P. Tipton,²⁵ A. Titov,²⁶ S. Tkaczyk,⁷ K. Tollefson,²⁵ A. Tollestrup,⁷ J. Tonnison,²⁴ J. F. de Troconiz,⁹ J. Tseng,¹² M. Turcotte,²⁹ N. Turini,² N. Uemura,³² F. Ukegawa,²¹ G. Unal,²¹ S. van den Brink,²² S. Vejcik, III,¹⁶ R. Vidal,⁷ M. Vondracek,¹⁰ R. G. Wagner,¹ R. L. Wagner,⁷ N. Wainer,⁷ R. C. Walker,²⁵ C. H. Wang,²⁸ G. Wang,²³ J. Wang,⁵ M. J. Wang,²⁸ Q. F. Wang,²⁶ A. Warburton,¹¹ G. Watts,²⁵ T. Watts,²⁷ R. Webb,³⁰ C. Wendt,³⁴ H. Wenzel,¹⁴ W. C. Wester, III,¹⁴ T. Westhusing,¹⁰ A. B. Wicklund,¹ E. Wicklund,⁷ R. Wilkinson,²¹ H. H. Williams,²¹ P. Wilson,⁵ B. L. Winer,²⁵ J. Wolinski,³⁰ D. Y. Wu,¹⁶ X. Wu,²³ J. Wyss,²⁰ A. Yagil,⁷ W. Yao,¹⁴ K. Yasuoka,³² Y. Ye,¹¹ G. P. Yeh,⁷ P. Yeh,²⁸ M. Yin,⁶ J. Yoh,⁷ T. Yoshida,¹⁹ D. Yovanovitch,⁷ I. Yu,³⁵ J. C. Yun,⁷ A. Zanetti,²³ F. Zetti,²³ L. Zhang,³⁴ S. Zhang,¹⁶ W. Zhang,²¹ and S. Zucchelli²

(CDF Collaboration)

¹ Argonne National Laboratory, Argonne, Illinois 60439

² Istituto Nazionale di Fisica Nucleare, University of Bologna, I-40126 Bologna, Italy

³ Brandeis University, Waltham, Massachusetts 02254

⁴ University of California at Los Angeles, Los Angeles, California 90024

⁵ University of Chicago, Chicago, Illinois 60637

⁶ Duke University, Durham, North Carolina 27708

- ⁷ *Fermi National Accelerator Laboratory, Batavia, Illinois 60510*
- ⁸ *Laboratori Nazionali di Frascati, Istituto Nazionale di Fisica Nucleare, I-00044 Frascati, Italy*
- ⁹ *Harvard University, Cambridge, Massachusetts 02138*
- ¹⁰ *University of Illinois, Urbana, Illinois 61801*
- ¹¹ *Institute of Particle Physics, McGill University, Montreal H3A 2T8, and University of Toronto, Toronto M5S 1A7, Canada*
- ¹² *The Johns Hopkins University, Baltimore, Maryland 21218*
- ¹³ *National Laboratory for High Energy Physics (KEK), Tsukuba, Ibaraki 305, Japan*
- ¹⁴ *Lawrence Berkeley Laboratory, Berkeley, California 94720*
- ¹⁵ *Massachusetts Institute of Technology, Cambridge, Massachusetts 02139*
- ¹⁶ *University of Michigan, Ann Arbor, Michigan 48109*
- ¹⁷ *Michigan State University, East Lansing, Michigan 48824*
- ¹⁸ *University of New Mexico, Albuquerque, New Mexico 87131*
- ¹⁹ *Osaka City University, Osaka 588, Japan*
- ²⁰ *Universita di Padova, Istituto Nazionale di Fisica Nucleare, Sezione di Padova, I-35131 Padova, Italy*
- ²¹ *University of Pennsylvania, Philadelphia, Pennsylvania 19104*
- ²² *University of Pittsburgh, Pittsburgh, Pennsylvania 15260*
- ²³ *Istituto Nazionale di Fisica Nucleare, University and Scuola Normale Superiore of Pisa, I-56100 Pisa, Italy*
- ²⁴ *Purdue University, West Lafayette, Indiana 47907*
- ²⁵ *University of Rochester, Rochester, New York 14627*
- ²⁶ *Rockefeller University, New York, New York 10021*
- ²⁷ *Rutgers University, Piscataway, New Jersey 08854*
- ²⁸ *Academia Sinica, Taiwan 11529, Republic of China*
- ²⁹ *Superconducting Super Collider Laboratory, Dallas, Texas 75237*
- ³⁰ *Texas A&M University, College Station, Texas 77843*
- ³¹ *Texas Tech University, Lubbock, Texas 79409*
- ³² *University of Tsukuba, Tsukuba, Ibaraki 305, Japan*
- ³³ *Tufts University, Medford, Massachusetts 02155*
- ³⁴ *University of Wisconsin, Madison, Wisconsin 53706*
- ³⁵ *Yale University, New Haven, Connecticut 06511*
- ^a *Visitor*

Abstract

We have used 19 pb^{-1} of data collected with the Collider Detector at Fermilab to search for new particles decaying to dijets. We exclude at 95% confidence level models containing the following new particles: axiglasons with mass between 200 and 870 GeV/c^2 , excited quarks with mass between 80 and 570 GeV/c^2 , and color octet

technirhos with mass between 320 and 480 GeV/c².

PACS numbers: 13.85.Rm, 12.38.Qk, 13.85.Ni, 13.87.Ce, 14.65.-q

Within the framework of perturbative QCD two-jet events are expected to arise in proton-antiproton collisions from hard parton-parton scattering. The outgoing scattered partons manifest themselves as hadronic jets. The predicted two-jet mass spectrum falls rapidly with increasing two-jet mass. Many extensions of the standard model predict the existence of new massive objects that couple to quarks and gluons, and result in resonant structures in the two-jet mass spectrum. In this paper we report a search for narrow resonances in the two-jet mass spectrum measured in proton-antiproton collisions at a center of mass energy $\sqrt{s} = 1.8$ TeV.

In addition to this general search, we specifically search for the following six resonance phenomena. First, in a model where the symmetry group $SU(3)$ of QCD is replaced by the chiral symmetry $SU(3)_L \times SU(3)_R$, there are axial vector particles called axigluons A [1]. The axigluon is produced and decays in the quark-antiquark channel ($A \rightarrow q\bar{q}$); here we have assumed they decay only to the quarks in the standard model. Second, if quarks are composite particles then excited states q^* are expected [2]; we search for mass degenerate excited quarks in the quark-gluon channel ($q^* \rightarrow qg$). Third, models of walking technicolor [3], which seek to explain electro-weak symmetry breaking via the dynamics of a new interaction among techniquarks,

predict the presence of color octet technirhos ρ_T . We consider such a model in which the ρ_T are mass degenerate and decay to dijets only ($\rho_T \rightarrow g \rightarrow q\bar{q}$ or gg); in this model the technipion is too massive to be a decay product of the ρ_T . Fourth and fifth, models which propose new gauge symmetries often predict new gauge bosons [4] which decay to quarks ($W', Z' \rightarrow q\bar{q}$). Here we assume standard model couplings and when calculating the cross section include a K-factor [5] to account for higher order terms. Finally, superstring theory suggests that E_6 may be the grand unified strong and electro-weak gauge group; E_6 models predict the presence of scalar diquarks D and D^c [6] which decay to quarks ($D \rightarrow \bar{u}\bar{d}$ and $D^c \rightarrow ud$). We assume electromagnetic strength couplings and mass degenerate diquarks.

A detailed description of the Collider Detector at Fermilab (CDF) can be found elsewhere [7]. We use a coordinate system with z along the proton beam, transverse coordinate perpendicular to the beam, azimuthal angle ϕ , polar angle θ , and pseudo-rapidity $\eta = -\ln \tan(\theta/2)$. Jets are reconstructed as localized energy depositions in the CDF calorimeters which are constructed in a tower geometry. The jet energy E and momentum \vec{P} are defined as the scalar and vector sums respectively of calorimeter tower energies inside a cone of radius $R = \sqrt{(\Delta\eta)^2 + (\Delta\phi)^2} = 0.7$ centered on the jet direction. E and \vec{P} are corrected for calorimeter non-linearities, energy lost in uninstrumented regions and outside the clustering cone, and energy gained from the underlying event. The jet energy corrections increase the jet energies on average by roughly 27%(15%) for 50 GeV (500 GeV) jets. Full details of jet reconstruction and jet energy corrections at CDF can be found elsewhere [8].

We define the dijet system as the two jets with the highest transverse momentum in the event (leading jets) and define the dijet mass $m = \sqrt{(E_1 + E_2)^2 - (\vec{P}_1 + \vec{P}_2)^2}$. The dijet mass resolution is approximately 10%. Our data sample was obtained in the 1992-93 running period using four single jet triggers with thresholds on the uncorrected cluster transverse energies of 20, 50, 70 and 100 GeV. After jet energy corrections these trigger samples were used to measure the dijet mass spectrum above 150, 241, 265, and 353 GeV/ c^2 respectively. At these mass thresholds the trigger efficiencies for the four triggers were 1.0, 0.99, 0.87, and 0.89, and the four data samples corresponded to integrated luminosities of 0.038, 0.66, 3.2, and 19.1 pb⁻¹ after prescaling. Offline we required that both jets have pseudorapidity $|\eta| < 2$ and a scattering angle in the dijet center of mass frame $|\cos\theta^*| = |\tanh[(\eta_1 - \eta_2)/2]| < 2/3$. The $\cos\theta^*$ cut provides uniform acceptance as a function of mass and reduces the QCD background which peaks at $|\cos\theta^*| = 1$. To maintain the projective nature of the calorimeter towers, the z position of the event vertex was required to be within 60 cm of the center of the detector; this cut was 94% efficient. Backgrounds from cosmic-ray interactions were rejected if the energy deposited in the central hadronic calorimeters occurred at times other than the the $p\bar{p}$ crossing. Remaining backgrounds from cosmic-rays, beam halo, and detector noise produced events with unusually large or unbalanced energy depositions and were removed by requiring $\cancel{E}_T/\sqrt{\sum E_T} < 6$ and $\sum E_T < 2$ TeV, where \cancel{E}_T is the missing transverse energy [9] and $\sum E_T$ is the total transverse energy in the event.

In Fig. 1 we present the inclusive dijet mass distribution for $p\bar{p} \rightarrow 2$ leading jets

+ X, where X can be anything including additional jets. The dijet mass distribution has been corrected for trigger and z vertex inefficiencies. We plot the differential cross section versus the mean dijet mass in bins equal to the dijet mass resolution (RMS \sim 10%). The data is compared to a QCD prediction [10] which includes a simulation of the CDF detector. The QCD prediction uses CTEQ2L parton distributions [11], a renormalization scale $\mu = P_T$, and is normalized to the data. We also fit the data with the parameterization $d\sigma/dm = A(1 - m/\sqrt{s})^N/m^P$ with parameters A, N and P. This parameterization gives a good description of both the observed distribution ($\chi^2/DF = .96$) and the QCD prediction ($\chi^2/DF = .75$). The fit to the observed distribution gave $A = (6.4 \pm 0.1) \times 10^{15}$ pb/(GeV/c²), $N = 5.512 \pm 0.002$, and $P = 6.69 \pm 0.09$, where the quoted errors are statistical only. Fig. 1 shows the background fit on a logarithmic scale, and Fig. 2 shows the fractional difference between the data and background fit on a linear scale. The fit shows no significant evidence for any new particle. Upward fluctuations appearing in the data near 250, 550 and 850 GeV/c² have statistical significance 2.3, 1.3 and 1.8 standard deviations when interpreted as “signals” for new particles at these masses. However, this minimal significance is reduced by roughly a factor of 2 after incorporating systematic uncertainties (discussed later).

To set limits on dijet resonances it is sufficient to determine the mass resolution for only one new particle type assuming each new particle’s natural half-width ($\Gamma/2$) is small compared to the dijet mass resolution. This is the case for these models of axiglions ($\Gamma/2M \approx 0.05$), excited quarks ($\Gamma/2M \approx 0.02$), color octet technirhos ($\Gamma/2M \approx 0.01$), new gauge bosons ($\Gamma/2M \approx 0.01$), and E_6 diquarks ($\Gamma/2M \approx 0.004$

for D and 0.001 for D^c). In Figs. 1 and 2 we show the predicted mass resolution for excited quarks (q^*) using the PYTHIA Monte Carlo [10] and a CDF detector simulation. The mass resolution has a Gaussian core ($\text{RMS}/M \sim 0.1$) from jet energy resolution and a long tail towards low mass from QCD radiation. We have used the q^* mass resonance curves in Figs. 1 and 2 to model the shape of all new particles decaying to dijets. As in our previous search for excited quarks [12], we perform a binned maximum likelihood fit of the data to both the background parameterization and the signal hypothesis. The method gave a Poisson likelihood as a function of the signal cross section. This was done independently at 20 different values of new particle mass from 200 to 1150 GeV/c^2 , resulting in 20 statistical likelihood distributions.

Systematic uncertainties on the cross section for observing a new particle in the CDF detector are shown in Fig. 2. Each systematic uncertainty on the fitted signal cross section was determined by varying the source of uncertainty by $\pm 1\sigma$ and re-fitting. In decreasing order of importance the sources of uncertainty are the 5% jet energy scale uncertainty, QCD radiation's effect on the mass resonance line shape, the background parameterization, trigger efficiency, jet energy resolution, jet energy scale of CDF calorimeters relative to the central calorimeter, luminosity and efficiency. For example, at 300 GeV/c^2 reducing the jet energy by 5% centers the resonance on an upward fluctuation, and increases the fitted signal by over 100%. The total systematic uncertainty was found by adding the above sources in quadrature. We convoluted each of the 20 likelihood distributions with the corresponding total Gaussian systematic uncertainty, and found the 95% confidence level (CL) upper limit shown in

Fig. 3.

In Fig. 3 and Table I we compare our measured upper limit on the cross section times branching ratio for a new particle decaying to dijets to the theoretical predictions. The predictions are lowest order with one-loop strong coupling $\alpha_s(m^2)$ and CTEQ2L parton distributions [11]. Branching fractions to top quarks are included but do not add to the dijet mass resonance cross section. New particle decay angular distributions are included, and we required $|\eta| < 2$ and $|\cos\theta^*| < 2/3$. We exclude at 95% CL new particles in mass regions for which the theory curve lies above our upper limit. For axiglouons [1] we exclude the region $200 < M_A < 870 \text{ GeV}/c^2$, significantly extending the previous CDF exclusions of $120 < M_A < 210 \text{ GeV}/c^2$ [13] and $240 < M_A < 640 \text{ GeV}/c^2$ [14] and the UA1 exclusion of $110 < M_A < 310 \text{ GeV}/c^2$ [15]. For the first time we exclude a model of technicolor [3] with color octet technirhos in the mass range $320 < M_{\rho_T} < 480 \text{ GeV}/c^2$. From Fig. 3 we exclude excited quarks in the mass range $200 < M^* < 560 \text{ GeV}/c^2$ at 95% CL. This limit from dijets can be improved by combining it with published limits in the γ +jet and the W+jet channel [12] (by multiplying the likelihood distributions). Combining all three channels excludes excited quarks in the mass interval $80 < M^* < 570 \text{ GeV}/c^2$ for standard model couplings. The excluded regions in the coupling [2] vs. mass plane are shown in Fig. 4 compared to previous excluded regions. The cross section for new gauge bosons and E_6 diquarks is too small to be excluded by our data.

In conclusion, the measured dijet mass spectrum is a smoothly falling distribution within statistics. We see no significant evidence for new particle production and set

limits on axigluons, excited quarks, and color octet technirhos.

We thank the Fermilab staff and the technical staffs of the participating institutions for their vital contributions. We also thank Ken Lane for providing software we used to calculate the technirho cross section. This work was supported by the U.S. Department of Energy and National Science Foundation; the Italian Istituto Nazionale di Fisica Nucleare; the Ministry of Science, Culture, and Education of Japan; the Natural Sciences and Engineering Research Council of Canada; the A. P. Sloan Foundation; and the Alexander von Humboldt-Stiftung.

References

- [1] P. Frampton and S. Glashow, *Phys. Lett.* **B190**, 157 (1987); J. Bagger, C. Schmidt & S. King, *Phys. Rev.* **D37**, 1188 (1988).
- [2] U. Baur, I. Hinchliffe & D. Zeppenfeld, *Int. J. Mod. Phys* **A2**, 1285 (1987); U. Baur, M. Spira & P. Zerwas, *Phys. Rev.* **D42**, 815 (1990).
- [3] K. Lane & M. Ramana, *Phys. Rev.* **D44**, 2678 (1991); E. Eichten & K. Lane, *Phys. Lett.* **B327**, 129 (1994).
- [4] F. Abe et al., Fermilab-PUB-94/198-E and Fermilab-PUB-94/268-E (both submitted to *Phys. Rev. Lett.*) and references therein.
- [5] V. Barger and R. Phillips, *Collider Physics* (Addison-Wesley, 1987), p. 233 and 248.

- [6] J. Hewett and T. Rizzo, Phys. Rep. **183**, 193 (1989) and references therein.
- [7] F. Abe et al., Nucl. Inst. and Meth. **A271**, 387 (1988).
- [8] F. Abe et al., Phys. Rev. **D45**, 1448 (1992).
- [9] F. Abe et al., Phys. Rev. Lett. **66**, 2951 (1992).
- [10] PYTHIA V5.6 by T. Sjostrand, CERN-TH-6488/92, May 1992.
- [11] J. Botts et al., Phys. Lett. **B304**, 159 (1993).
- [12] F. Abe et al., Phys. Rev. Lett. **72**, 3004 (1994).
- [13] F. Abe et al., Phys. Rev. **D41**, 1722 (1990).
- [14] F. Abe et al., Phys. Rev. Lett. **71**, 2542 (1993).
- [15] C. Albajar et al., Phys. Lett. **B209**, 127 (1988).
- [16] D. Decamp et al., Phys. Rep. **216**, 253 (1992); J. Alitti et al., Nucl. Phys. **B400**, 3 (1993).

Mass GeV/c ²	95% CL σ .B Limit (pb)	Theory Cross Section \times Branching Ratio					
		A (pb)	q^* (pb)	ρ_T (pb)	W' (pb)	Z' (pb)	$D + D^c$ (pb)
200	4.2×10^3	1.0×10^4	8.6×10^3	1.5×10^3	4.1×10^2	1.9×10^2	6.3×10^2
250	1.3×10^3	4.7×10^3	2.9×10^3	5.3×10^2	1.7×10^2	9.2×10^1	2.4×10^2
300	4.0×10^2	2.4×10^3	1.1×10^3	2.2×10^2	7.8×10^1	4.7×10^1	9.8×10^1
350	4.8×10^1	1.3×10^3	4.5×10^2	1.0×10^2	3.8×10^1	2.6×10^1	4.3×10^1
400	1.9×10^1	6.8×10^2	1.9×10^2	5.2×10^1	1.9×10^1	1.4×10^1	1.9×10^1
450	1.5×10^1	3.8×10^2	8.7×10^1	2.7×10^1	1.0×10^1	8.0	8.9
500	2.1×10^1	2.1×10^2	4.0×10^1	1.4×10^1	5.6	4.4	4.2
550	1.7×10^1	1.2×10^2	1.9×10^1	7.3	3.2	2.6	2.0
600	1.2×10^1	6.8×10^1	8.9	3.8	1.7	1.5	9.2×10^{-1}
650	7.0	3.8×10^1	4.2	2.0	9.4×10^{-1}	8.6×10^{-1}	4.3×10^{-1}
700	4.1	2.2×10^1	2.0	1.1	5.1×10^{-1}	4.9×10^{-1}	2.0×10^{-1}
750	3.7	1.2×10^1	9.7×10^{-1}	5.5×10^{-1}	2.8×10^{-1}	2.7×10^{-1}	9.0×10^{-2}
800	3.5	6.7	4.6×10^{-1}	2.8×10^{-1}	1.5×10^{-1}	1.5×10^{-1}	4.0×10^{-2}
850	2.9	3.6	2.2×10^{-1}	1.4×10^{-1}	7.9×10^{-2}	8.5×10^{-2}	1.7×10^{-2}
900	2.4	1.9	1.0×10^{-1}	6.9×10^{-2}	4.1×10^{-2}	4.6×10^{-2}	7.3×10^{-3}
950	1.9	1.0	4.6×10^{-2}	3.3×10^{-2}	2.1×10^{-2}	2.4×10^{-2}	3.0×10^{-3}
1000	1.2	5.1×10^{-1}	2.1×10^{-2}	1.6×10^{-2}	–	–	–
1050	8.1×10^{-1}	2.4×10^{-1}	9.4×10^{-3}	–	–	–	–
1100	5.8×10^{-1}	1.2×10^{-1}	4.2×10^{-3}	–	–	–	–
1150	4.5×10^{-1}	5.2×10^{-2}	1.8×10^{-3}	–	–	–	–

Table I: As a function of new particle mass we list our 95% CL upper limit on cross section times branching ratio and the theoretical prediction for axigluons (A), excited quarks (q^*), color octet technirhos (ρ_T), new gauge bosons (W' and Z'), and E_6 diquarks ($D + D^c$). The limit and predictions require that both jets have pseudorapidity $|\eta| < 2.0$ and the dijet satisfies $|\cos\theta^*| < 2/3$.

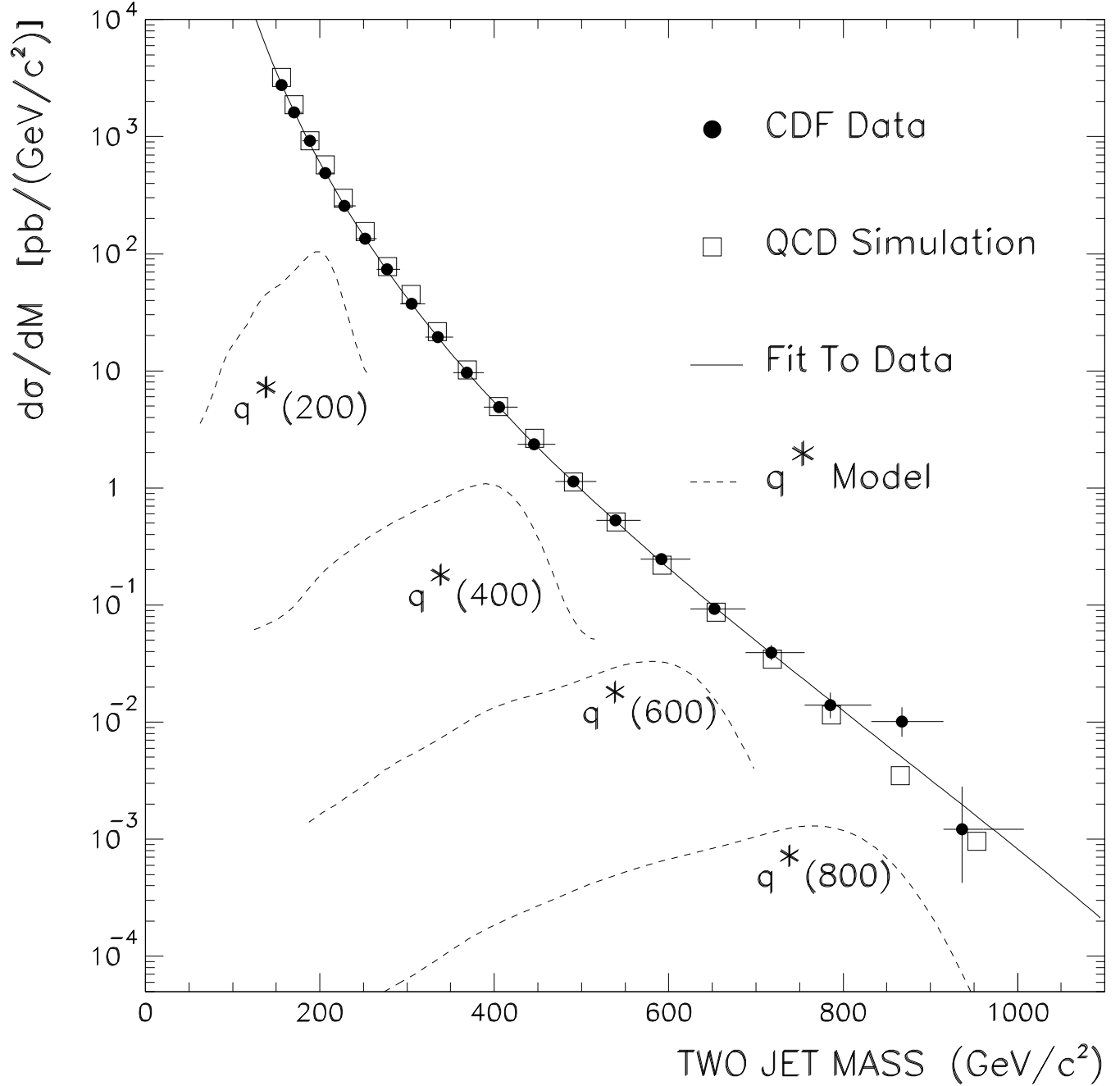


Figure 1: The dijet mass distribution (circles) compared to a QCD simulation (boxes) and fit to a smooth parameterization (solid curve). Also shown are simulations of excited quark signals in the CDF detector (dashed curves). In the data and simulations we require that both jets have pseudorapidity $|\eta| < 2.0$ and the dijet satisfies $|\cos\theta^*| < 2/3$.

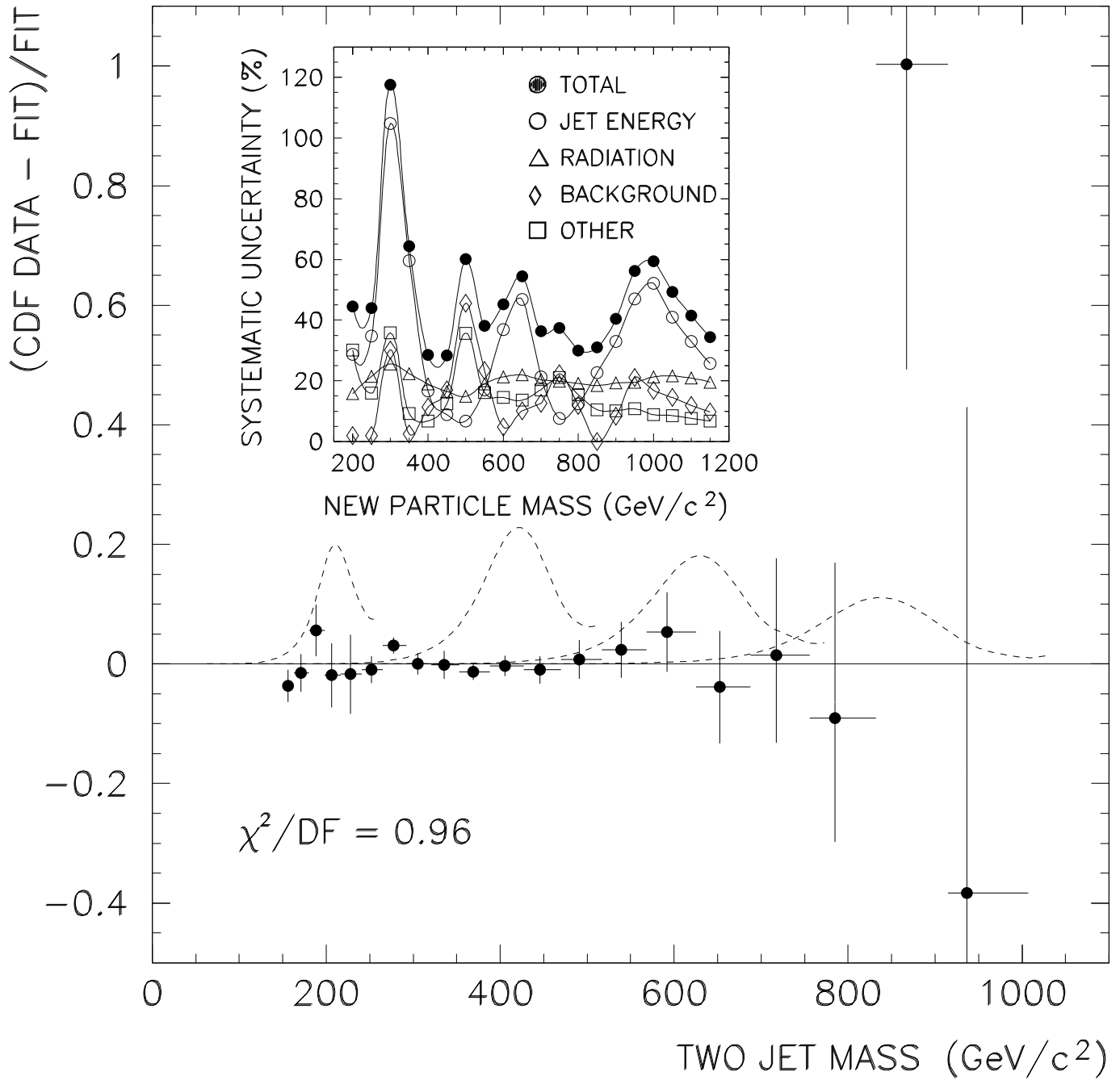


Figure 2: The fractional difference between the dijet mass distribution (points) and a smooth background fit (solid line) is compared to simulations of excited quark signals in the CDF detector (dashed curves). The inset shows the systematic uncertainty for a new particle signal (see text).

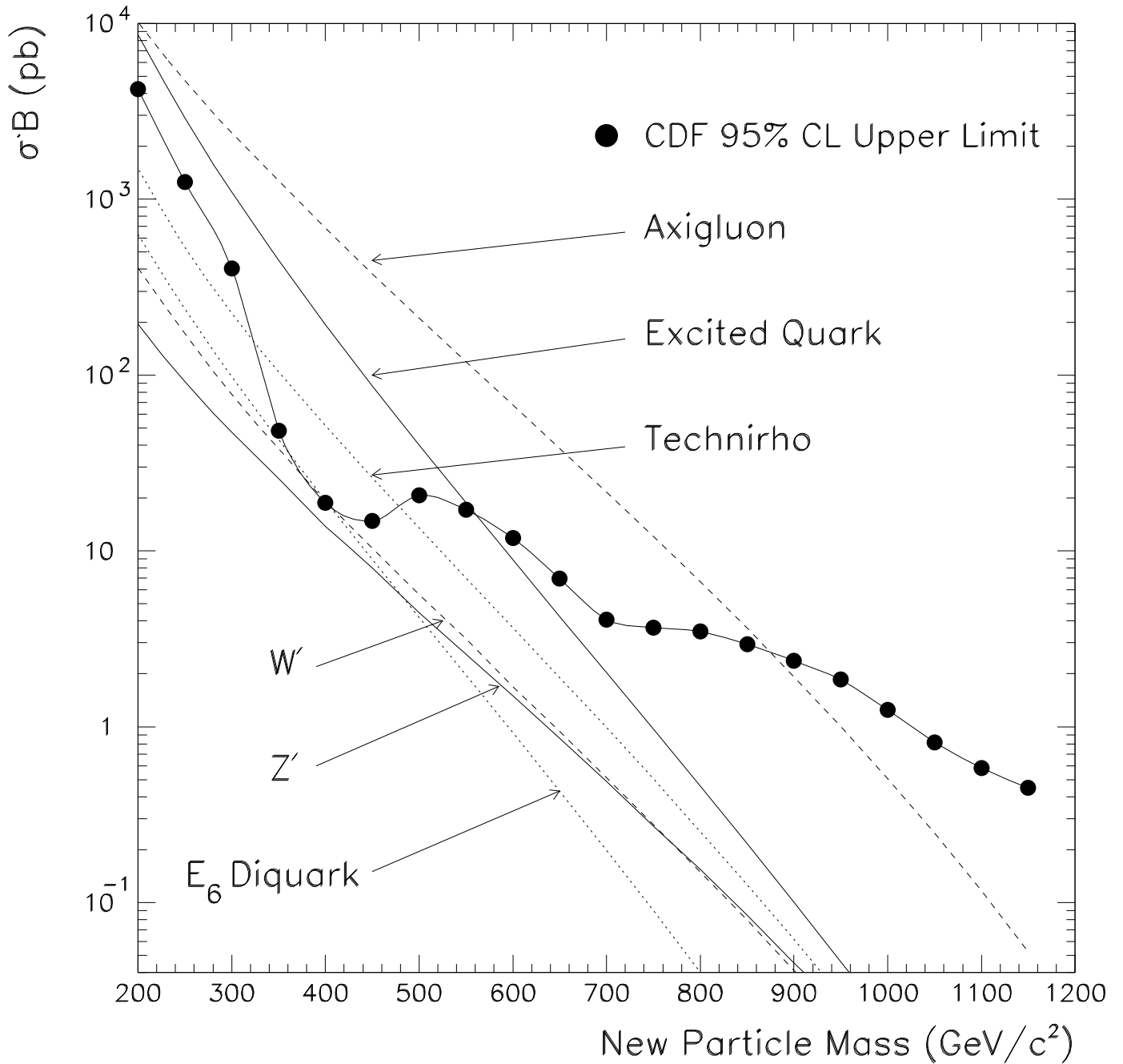


Figure 3: The upper limit on the cross section times branching ratio for new particles decaying to dijets (points) is compared to theoretical predictions for axigluons [1], excited quarks [2], color octet technirhos [3], new gauge bosons W' and Z' [4, 5], and E_6 diquarks [6]. The limit and theory curves require that both jets have pseudorapidity $|\eta| < 2.0$ and the dijet satisfies $|\cos \theta^*| < 2/3$.

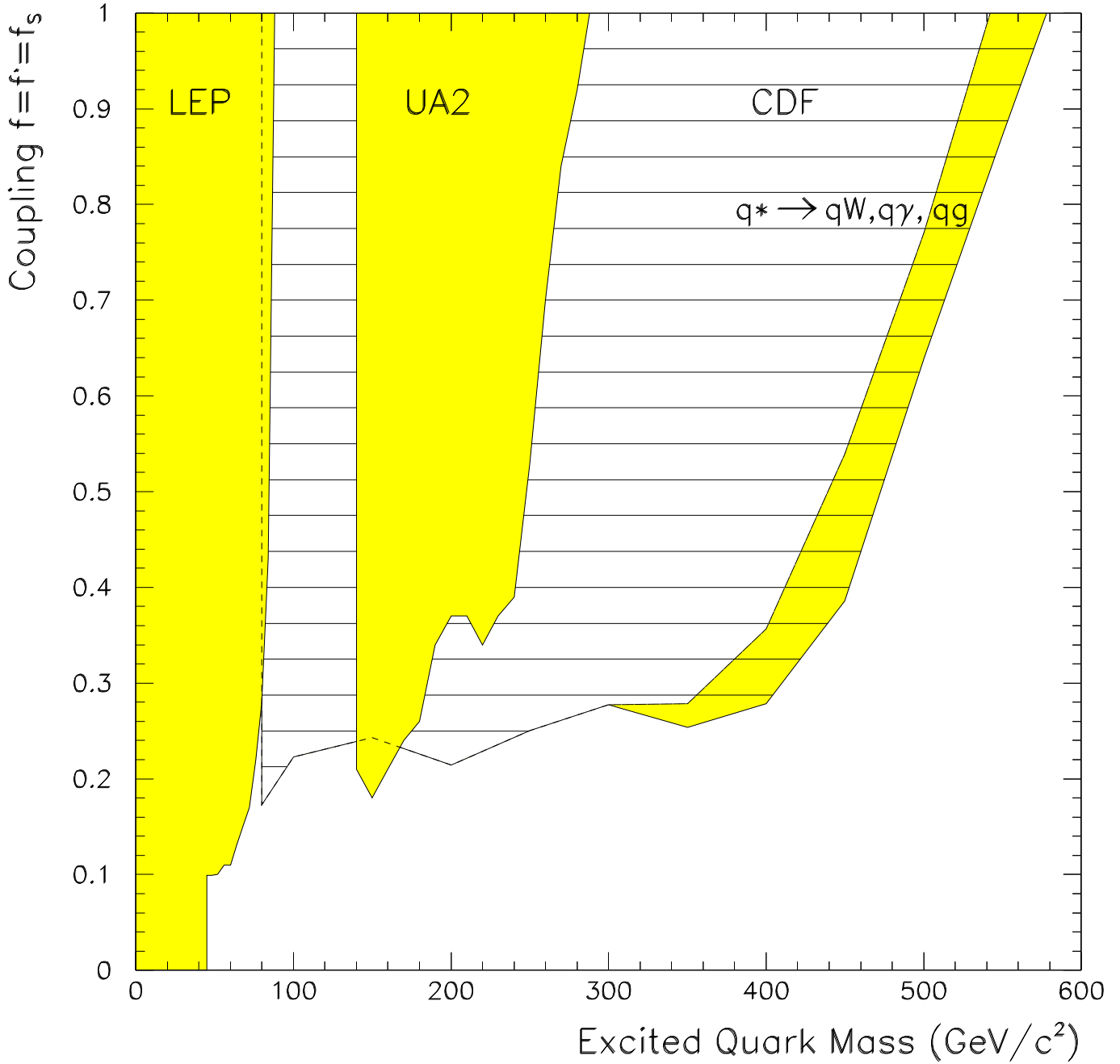


Figure 4: The region of the coupling vs. mass plane excluded by previous CDF measurements [12] in the $q^* \rightarrow q\gamma$ and $q^* \rightarrow qW$ channels (hatched region) is extended by combining them with this search in the $q^* \rightarrow qg$ channel (shaded and hatched region). The CDF excluded regions are compared to the regions excluded by LEP and UA2 (shaded regions) [16].

This figure "fig1-1.png" is available in "png" format from:

<http://arxiv.org/ps/hep-ex/9501001v2>

This figure "fig1-2.png" is available in "png" format from:

<http://arxiv.org/ps/hep-ex/9501001v2>

This figure "fig1-3.png" is available in "png" format from:

<http://arxiv.org/ps/hep-ex/9501001v2>

This figure "fig1-4.png" is available in "png" format from:

<http://arxiv.org/ps/hep-ex/9501001v2>